JPE 6-1-2

A Realization Method of Fault-tolerant Control of Flexible Arm under Sensor Fault by Using an Adaptive Sensor Signal Observer

Yu Izumikawa†, Kazuhiro Yubai* and Junji Hirai*

†*Dept. of Electrical and Electronic Eng., Mie University, Mie, Japan

ABSTRACT

In this paper, we propose a fault-tolerant control system for the position control and vibration suppression of a flexible arm robot. The proposed control system has a strain gauge sensor signal observer based on a reaction force observer and detects a fault by monitoring an estimated error. In order to improve the estimation accuracy, the plant parameters included in the sensor signal observer are updated by using the strain gauge sensor signal in normal time through the adaptive law. After fault detection, the proposed control system exchanges the faulty sensor signal for the estimated one and switches to a fault mode controller so as to maintain the stability and the control performance. We confirmed the effectiveness of the proposed control system through several experiments.

Keywords: fault-tolerance, sensor fault, flexible arm, reaction force estimation

1. Introduction

In recent years, control system reliability has received much attention with the increase of situations where robots are used. In order to improve reliability, control systems need to have the ability to detect a fault (fault detection) and to maintain stability and control performance (fault tolerance). In mechanical systems, actuator faults and sensor faults, which is the emphasis of this paper, are often concerned.

Many studies have been done on fault-tolerant control systems for sensor fault, and they are mainly classified into two approaches:

i. Design a controller which stabilizes both a normal and a faulty system by solving a robust stability problem or a simultaneous stabilization problem [1, 2].
ii. Estimate a faulty sensor signal from normal sensor signals, and use the estimated signal instead of a faulty one [3].

The first approach tends to be conservative since a (single) controller is designed for large model uncertainty to guarantee the stability of a normal and a faulty system. On the other hand, in the second approach, which exploits sensor redundancy, stability and control performance can be maintained by exchanging a faulty sensor signal for an estimated one reconstructed from input signals and normal sensor signals by utilizing interrelations of each sensor signal. However, from a practical point of view, the second approach lacks estimation robustness against plant deviations and disturbances. In this paper, we extend this approach by implementing a sensor signal observer, which has adaptive parameters, to overcome this problem.

This paper is concerned with the vibration suppression

Manuscript received May 31, 2005; revised Sept. 20, 2005
†Corresponding Author: izumi@ems.elec.mie-u.ac.jp
Tel: +81-59-231-9674, Fax:+81-59-231-9442, Mie Univ.
*Dept. of Electrical and Electronic Eng., Mie Univ.

control of a one-link flexible arm robot. In our control system, vibration suppression is realized by the additional feedback of a strain gauge sensor attached to the arm beside the motor angle. However, a sensor fault may degrade the control performance and make the control system unstable at its worst. In our control system, a strain gauge sensor is prone to fail in comparison with an encoder because it is attached directly to the arm. Therefore, we propose a fault-tolerant control system for a disconnection fault of a strain gauge sensor. We focus on a reaction force observer and show that a strain gauge sensor signal can be estimated by multiplying an appropriate gain to reaction force. Moreover, an adaptation algorithm is applied to update the plant parameters of the observer to improve estimation accuracy and estimation robustness. A strain gauge sensor fault is detected by monitoring an estimation error between the sensor signal and an estimated value, and the control system works with the estimated one after fault detection. However, the control system may be unstable after exchanging the sensor signal for the estimated one since the estimated value includes estimation error and estimation delay, and these effects are not considered at the controller design. Therefore, a fault-mode controller taking into account the estimation error and the estimation delay should be designed and the control systems should switch from the normal-mode controller to the fault-mode controller after fault detection to maintain the stability and the control performance. Loop Shaping Design Procedure (LSDP) is adopted as a controller synthesis to design both the normal-mode and the fault-mode controller. Both controllers are designed according to the same controlled plant with different weighting functions in consideration of the estimation error and the estimation delay. Thus, it is possible to design the fault-mode controller easily in comparison with constructing another sensor-less control system instead of the fault-mode controller.

The rest of this paper is organized as follows. Section 2 describes a mathematical model of a flexible arm robot and the vibration suppression control system. In section 3, a new fault-tolerant control system consisting of a sensor signal observer, an adaptation algorithm, switching controllers, and a fault detector is proposed. The effectiveness of the proposed fault-tolerant control system is examined through experiments in section 4. Section 5 concludes this paper.

2. Mathematical Model of Flexible Arm and Vibration Suppression Control System Configuration

The configuration of the one-link flexible arm used in our study is depicted in Fig. 1. The flexible arm has an encoder and a strain gauge sensor to detect motor angle and distortion of the arm. The Bernoulli-Euler beam theory and some simplifications give the mathematical model an input torque τ^{ref} to motor angle θ and to distortion of the arm S_d written as (1) and (2), respectively. In these equations, the higher order vibrations are neglected for simplicity of the controller design.

$$P_\theta = \frac{\theta}{\tau^{ref}} = \frac{1}{J_t}\left\{\frac{1}{s^2} + \frac{(\phi'(0))^2}{s^2+\omega^2}\right\} \tag{1}$$

$$P_{S_d} = \frac{S_d}{\tau^{ref}} = \frac{1}{J_t}\left\{\frac{\phi'(0)\phi''(x_s)}{s^2+\omega^2}\right\} \tag{2}$$

s : Laplace operator
x : distance from the root of arm
J_t : total moment of inertia
ω : resonant frequency of arm
ϕ : mode function

The strain gauge sensor is placed at the node of the second order vibration mode ($x=x_s$) so as to mainly detect the first order vibration mode. Vibration suppression control and tip position control are realized by feedback of the distortion of the arm S_d and motor angle θ through an appropriate stabilizing controller C_N[4].

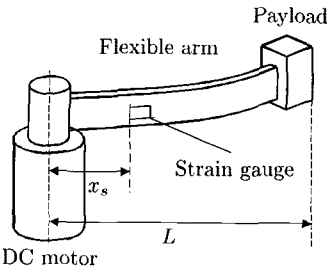

Fig. 1 Configuration of the one-link flexible arm

3.Proposed Control System

Since the control system of the flexible arm has no alternate for an encoder, the control system has to stop the operation immediately after fault detection in an encoder. In the case of a strain gauge sensor fault, it is possible to maintain the stability of the control system by interrupting the faulty sensor signal with an additional strain gauge. However, this interruption results in poor vibration suppression. In the control system of the flexible arm, it is desirable to maintain not only the stability of the control system, but also a vibration suppression performance after a strain gauge sensor fault. For this purpose, we propose a new fault-tolerant control system

- To estimate a strain gauge sensor signal,
- To detect a fault and exchange a faulty sensor signal for the estimated one, and
- To maintain a stability and a control performance after switching from a faulty sensor signal to the estimated one.

Figure 2 illustrates the configuration of the proposed fault-tolerant control system. The proposed system is constructed by adding a strain gauge sensor signal observer, an adaptive algorithm, a fault-mode controller C_F, and a fault detector to the (normal) control system of the flexible arm. The rest of this section describes the details of these components.

3.1 Sensor signal observer

A sensor signal observer estimates a strain gauge sensor signal from a reaction force estimated by a reaction force observer. In this section, we first give a brief review of the reaction force observer proposed in [5]. Secondly, we introduce the relationship between a reaction force and a strain gauge sensor signal, and show that the strain gauge sensor signal can be constructed from a reaction force. Furthermore, the plant parameters of the sensor signal observer are updated to improve estimation accuracy and estimation robustness against disturbances and parameter variations.

3.1.1 Estimation of strain gauge sensor signal

A reaction force observer is proposed to estimate the

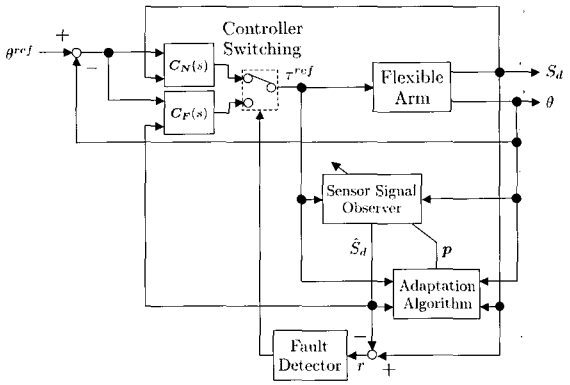

Fig. 2 Proposed fault-tolerant control system

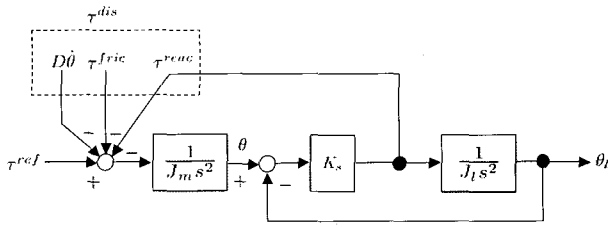

Fig. 3 A model of 2-mass resonant system

reaction force τ^{ref} acting on a motor in a 2-mass resonant system as shown in Fig. 3, and some successful applications are reported (e.g., vibration suppression control of 2-mass resonant system[5] and sensor-less force control[6]). In Fig. 3, the transfer function from input torque τ^{ref} to motor position θ is written as

$$\frac{\theta}{\tau^{ref}} = \frac{1}{J_m s^2}\left\{\frac{s^2 + K_s/J_l}{s^2 + (J_m + J_l)K_s/J_m J_l}\right\} \tag{3}$$

By comparing (3) with (1), a flexible arm can be modeled as a 2-mass resonant system with an equivalent motor inertia J_m, an equivalent load inertia J_l, and an equivalent spring coefficient K_s as defined from (4) to (6), respectively [7].

$$J_m = \frac{J_t}{1+\phi'(0)^2} \tag{4}$$

$$J_l = \frac{J_t \phi'(0)^2}{1+\phi'(0)^2} \tag{5}$$

$$K_s = \frac{J_t \phi'(0)^2 \omega^2}{\left(1+\phi'(0)^2\right)^2} \tag{6}$$

Assume that a disturbance torque τ^{dis} entering at a motor input is composed as (7), where D and τ^{fric} are motor viscosity and friction torque, respectively.

$$\tau^{dis} = Ds\theta + \tau^{fric} + \tau^{reac} \tag{7}$$

Another expression of τ^{dis} is obtained from Fig. 3 as follows:

$$\tau^{dis} = \tau^{ref} - J_m s^2 \theta \tag{8}$$

From (7) and (8), a reaction force τ^{reac} is estimated by

$$\hat{\tau}^{reac} = F\left(\tau^{ref} - J_m s^2\theta - Ds\theta - \hat{\tau}^{fric}\right) \tag{9}$$

where F is the second order low-pass filter in order to avoid pure derivation of θ and suppress the effect of the neglected higher order vibration modes. The cut-off frequency of F is determined as 300[rad/s] in consideration of the fact that the neglected vibration modes exist higher than 300[rad/s]. Furthermore, $\hat{\tau}^{fric}$ is defined as follows:

$$\hat{\tau}^{fric} = \begin{cases} \tau^c \operatorname{sgn}(\dot{\theta}) & : \text{if } |\dot{\theta}| > \alpha \\ \tau^{ref} \operatorname{sgn}(\dot{\theta}) & : \text{if } |\dot{\theta}| > \alpha \text{ and } |\tau^{ref}| > \tau^s \\ \tau^{ref} & : \text{if } |\dot{\theta}| < \alpha \text{ and } |\tau^{ref}| \le \tau^s \end{cases} \tag{10}$$

where τ^c, τ^s, and α denote the coulomb friction torque, the static friction torque, and the minimum resolution of $\dot{\theta}$, respectively.

From Fig. 3, the transfer function from τ^{ref} to τ^{reac} are written as

$$\frac{\tau^{reac}}{\tau^{ref}} = \frac{K_s/J_m}{s^2 + (J_m + J_l)K_s/J_m J_l} = \frac{\phi'(0)^2\omega^2/(1+\phi'(0)^2)}{s^2+\omega^2} \tag{11}$$

Comparing (2) with (11) yields the following relationship between τ^{reac} and S_d:

$$S_d = \frac{(1+\phi'(0)^2)\phi''(x_s)}{J_l\phi'(0)\omega^2}\tau^{reac} = K\tau^{reac} \tag{12}$$

From (9) and (12), S_d can be estimated by (13) from only available signals, θ and τ^{ref}.

$$\hat{S}_d = K\hat{\tau}^{reac} = KF\left(\tau^{ref} - J_m s^2\theta - Ds\theta - \hat{\tau}^{fric}\right) \tag{13}$$

A configuration of the sensor signal observer is shown in Fig. 4.

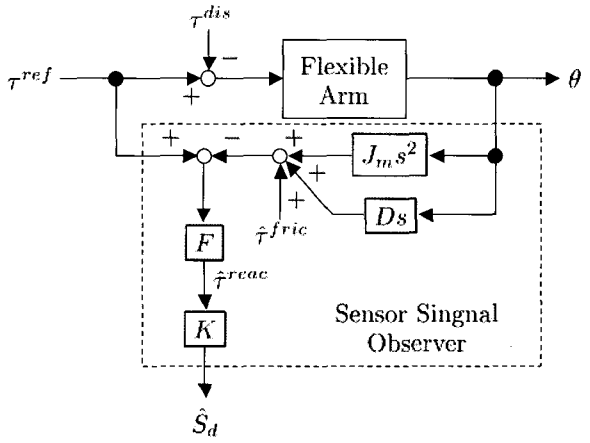

Fig. 4 Sensor signal observer

3.1.2 Parameter adaptation

The sensor signal observer contains unknown parameters such as J_m, K, D, τ^c, and τ^s. In these parameters, J_m and K can be determined by (4) and (12) analytically, while D, τ^c, and τ^s should be obtained by preliminary identification. However, plant deviations, disturbances and inevitable identification errors on these plant parameters may result in the poor estimation of S_d. In order to improve estimation accuracy, the plant parameters of the sensor signal observer are updated in normal time by regarding S_d as a teaching signal.

The parameter vector $\boldsymbol{p}$ and the regressor ξ are defined as (14) and (15), respectively.

$$\boldsymbol{p} = \left[K, -KJ_m, -KD, -K\tau^c\right]^T \tag{14}$$

$$\xi = F\left[\tau^{ref}, \ddot{\theta}, \dot{\theta}, \operatorname{sgn}(\dot{\theta})\right]^T \tag{15}$$

$\boldsymbol{p}$ is estimated from the regression model as follows:

$$S_{dF} = \xi^T \boldsymbol{p} \tag{16}$$

Where S_{dF} is defined as FS_d. we adopt a discontinuous projection algorithm and constant-trace algorithm[8] as the parameter adaptation algorithm shown in (17), (18), and (19).

$$\dot{\boldsymbol{p}} = \mathrm{Pr}_p\left[\Gamma\xi\left(S_{dF} - \xi^T \boldsymbol{p}\right)\right] \tag{17}$$

$$\mathrm{Pr}_p[\bullet_i] = \begin{cases} 0 & \text{if } p_i = \overline{p_i} \ \& \ \bullet_i > 0 \\ 0 & \text{if } p_i = \underline{p_i} \ \& \ \bullet_i > 0 \\ \bullet_i & \text{otherwise} \end{cases} \tag{18}$$

$$\dot{\Gamma} = \frac{|\Gamma\xi|^2}{\mathrm{Tr}(\Gamma[0])}\Gamma - \Gamma\xi\xi^T\Gamma \tag{19}$$

$\overline{p_i}$ and $\underline{p_i}$ denote the prespecified upper and lower bound of p_i, respectively. The parameter adaptation is activated only in fault-free time since wrong information is obtained after a sensor fault occurs. Only τ^s is identified in advance and is restricted to be constant since the lack of persistency exciting measurement in $\dot{\theta} \cong 0$ leads to poor estimation of τ^s and τ^s can be obtained easily by preliminary identification in comparison with the other parameters.

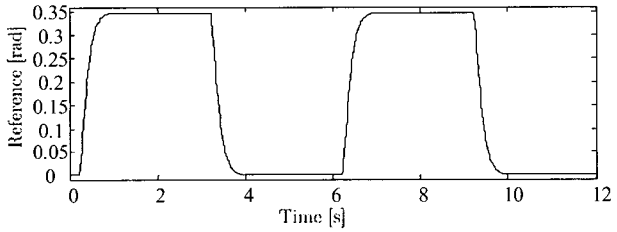

Fig. 5 Reference

Table 1 Plant parameters

symbol	description	value
L	Length of arm	0.493 [m]
J_t	Total moment of inertia	0.7326[kg · m^2]
ω	Resonant frequency	27.08 [rad/m]
τ^s	Static friction torque	13.4125 [Nm]
$\phi'(0)$	First derivative of mode function with respect to x at x=0	0.6365
$\phi''(x_s)$	Second derivative of mode function with respect to x at $x = x_s$	-9.4814

3.1.3 Sensor signal estimation results

We have performed the strain gauge sensor signal estimation by the sensor signal observer. The flexible arm is controlled by a stabilizing controller and a filtered step signal shown in Fig. 5 is added as a reference. All components of $\boldsymbol{p}$ are initially set to zero. Plant parameters obtained by preliminary identification are listed in Table 1.

Figures 6 and 7 depict the transition of $\boldsymbol{p}$ and the sensor signal estimation result after convergence of $\boldsymbol{p}$, respectively. These results show that each parameter p_i converges to a constant value and the sensor signal observer estimates S_d well after convergence of $\boldsymbol{p}$. However, these estimation results include estimation error and estimation delay caused by modeling error and the filter F attached to the sensor signal observer. The control system may be unstable after exchanging the sensor signal for the estimated one. This is the reason why a fault-mode controller activated after fault detection should be designed to maintain stability and control performance.

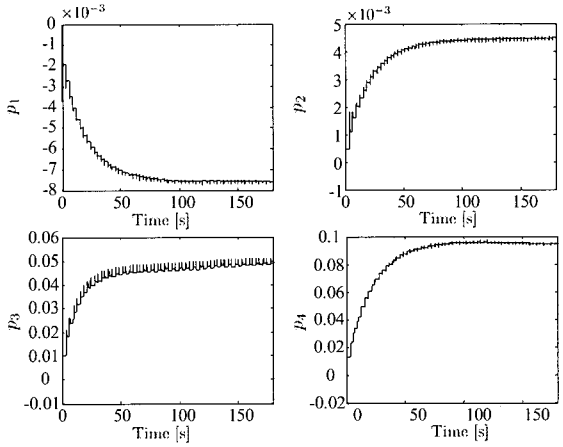

Fig. 6 Transition of p

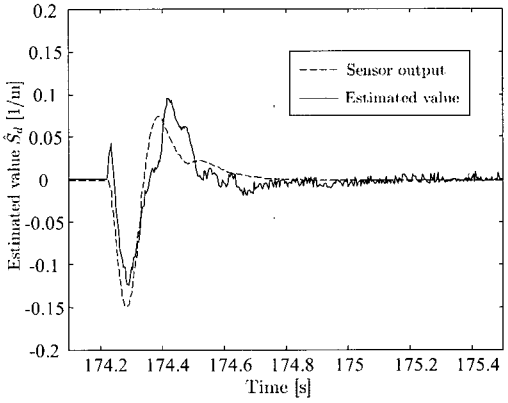

Fig. 7 Sensor signal estimation result

3.2 Controller design

Loop Shaping Design Procedure (LSDP) is adopted as a controller synthesis to design the normal-mode controller C_N and the fault-mode controller C_F. In this procedure, the open-loop characteristics of the controlled plant $P=[P_\theta, P_{S_d}]^T$ are shaped by a precompensator V and a postcompensator W=diag(W_1, W_2). A stabilizing controller C_∞ which guarantees robust stability margin and the specified open-loop characteristics is designed for the shaped plant G=WPV by solving two Riccati equations, see [9] for details. The resulting feedback controller for the controlled plant P is constructed as

$$C = VC_\infty W \tag{20}$$

We adopt LSDP from the following reasons:

i. Loop-shaping by V and W needs no consideration on phase characteristics.
ii. Since both input and output sensitivities can be considered simultaneously, it is suitable for a controlled plant with a bad condition number, such as a flexible arm.
iii. Weighting functions are determined easily in comparison with H_∞ control because the LSDP is based on loop-shaping in open-loop as well as classical loop-shaping.

The third feature, especially, allows for the intuitive selection of weighting functions when designing C_N and C_F. While the weighting functions V and W for C_N are specified so as to satisfy given control requirements without consideration of any faults, C_F must be designed in consideration of the estimation error and the estimation delay caused by F. In order to specify V and W for C_F, the power spectrum densities of S_d and $\hat{S}_d$ are examined. Figure 8 illustrates the power spectrum densities of S_d and $\hat{S}_d$ whose waveform is presented in Fig. 7. The power spectrum density of $\hat{S}_d$ is larger than that of S_d by about 55[rad/s]. This implies that the estimation error is significantly higher than 55[rad/s]. Thus, only W_2 is modified so that the open loop gain of $W_2 P_{S_d} V$ indicates lower gain than the fault-free scenario in higher than 55[rad/s] at designing C_F to maintain the stability of the control system, while V and W_1 are identical to those for C_N. Table 2 shows the weighting functions V and W for C_N and C_F determined based on the above observation. Moreover, the low-pass filter F is added to W_2 C_F in consideration of the estimation delay of $\hat{S}_d$, and hence C_∞ in designing C_F is designed based on P shaped by V and $W' = \mathrm{diag}(W_1, FW_2)$. However, the resulting feedback controller C_F is constructed according to (20) by using $W = \mathrm{diag}(W_1, W_2)$ since the sensor signal observer includes F. Bode diagrams of C_N and C_F are shown in Fig. 9. C_F is designed so as to indicate lower gain, especially from S_d to τ^{ref}, than C_N in high frequencies considering estimation error between S_d and $\hat{S}_d$, while the bode diagram from θ to τ^{ref} changes little. From Fig. 9, it is expected that the control system after fault maintains tracking and vibration suppression performance and has robustness against estimation error and estimation delay.

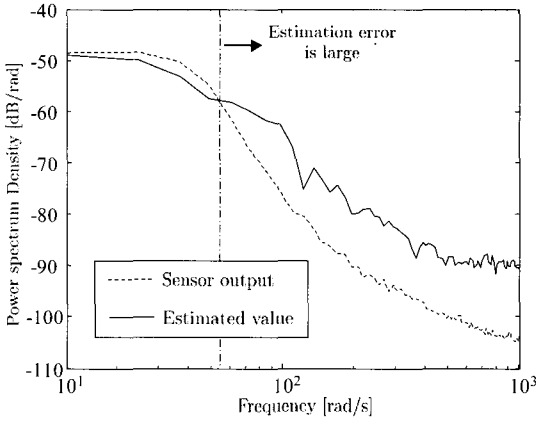

Fig. 8 Power spectrum density of S_d and $\hat{S}_d$

Table 2 Weighting functions V, W_1, and W_2

	for C_N	for C_F
V	$\frac{500s+250000}{s^2+1000s}$	
W_1	$\frac{264400s^2+23280000s+128500000}{s^2+1000s+250000}$	
W_2	$\frac{-4877s+166000}{s+500}$	200

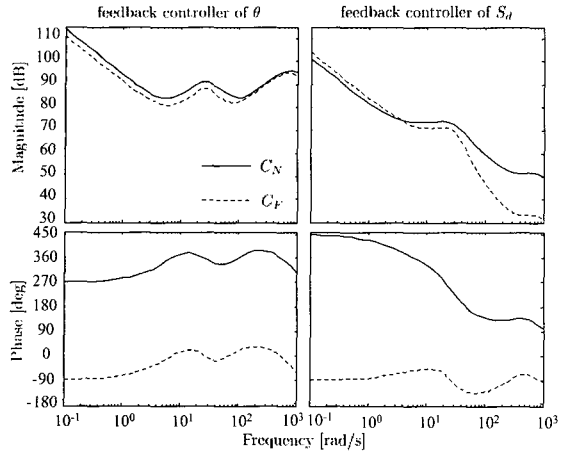

Fig. 9 Bode diagrams of C_N and C_F

Moreover, in order to avoid control performance degradation caused by discontinuous τ^{ref} at controller switching from C_N to C_F, an initial state of C_F should be set appropriately so that an output of C_F coincides with that of C_N at the controller switching [10].

3.3 Fault detector

In order to switch the controller, the control system has to detect when the fault occurs. The residual signal, which is the index of fault detection, should be nearly zero during fault-free, and be nonzero under faulty situations [11]. In this paper, we assume the faulty sensor signal deviates largely from the normal one at disconnection fault as stated in [12]. Since a complex fault detection scheme is not required under this assumption, we adopted an estimation error between the sensor signal S_d and the estimated value $\hat{S}_d$ as the residual signal r as

$$r = S_d - \hat{S}_d \tag{21}$$

The fault detector calculates r at each control period, and detects the fault as soon as the residual signal exceeds the prespecified threshold r_{th}.

4. Experimental Results

In order to verify the effectiveness of the proposed fault-tolerant control system, a disconnection fault of the strain gauge sensor was simulated after convergence of p. In this experiment, disconnection fault occurs virtually at 180.35[s], and the faulty sensor indicates 1.0[1/m], which is much larger than the fault-free scenario, after the disconnection fault occurrence [12]. The threshold r_{th} is set to ± 0.2[1/m] for the disconnection fault.

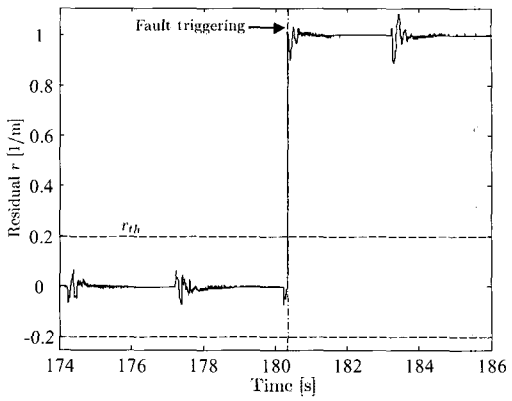

Fig. 10 Residual signal r

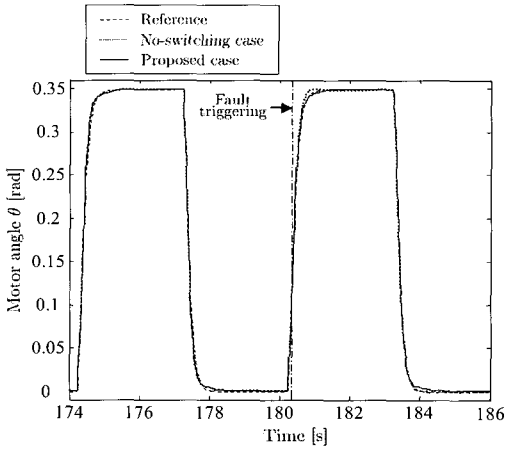

Fig. 11 Motor angle θ

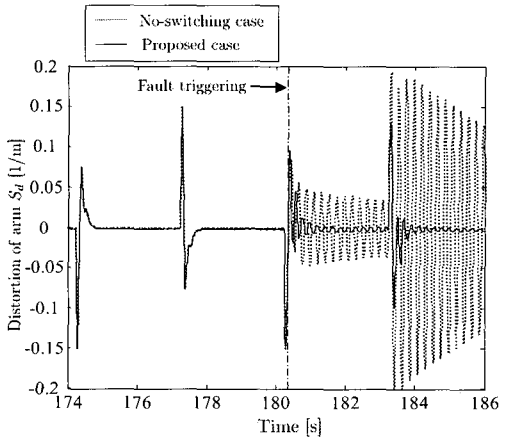

Fig. 12 Distortion of arm S_d

The residual signal r, depicted in Fig. 10, is nearly equal to zero when there is no fault. Once fault occurs, r exceeds r_{th}, and the fault detector immediately indicates the occurrence of the train gauge sensor fault. Figures 11 and 12 show the motor angle θ and the distortion of the arm S_d, respectively, together with the no-switching case for comparison. A no-switching case means that only an interruption of a faulty sensor signal is performed. The tracking performance associated with the motor angle θ has little degradation. While the vibration suppression performance degrades a lot in the no-switching case, the proposed case shows enough vibration suppression close to the fault-free scenario. These results show that the proposed fault-tolerant control system maintains the stability and the overall performance after the strain gauge sensor fault.

Table 3 Plant parameters (load increase case)

symbol	Value
J_t	0.8733 [kg · m^2]
ω	22.93 [rad/s]
$\phi'(0)$	0.8446
$\phi''(x_s)$	-8.8846

Next, the same experiments were examined with an unknown load at the tip of the arm to confirm robustness against plant deviation. Table 3 shows the plant parameters after the load increase (about 0.5[kg]). In this case, all components of $\boldsymbol{p}$ obtained before load change are not optimal since the increase of J_t causes variations of ω and ϕ, and consequently leads to a variation of K. The initial $\boldsymbol{p}$ is set to the value obtained in the experimental result shown in Fig. 6. The transition of $\boldsymbol{p}$ and the sensor signal estimation results are depicted in Figs. 13 and 14. Figure 14 includes the results with the fixed $\boldsymbol{p}$ for comparison. $\boldsymbol{p}$ converges to a different value obtained in the previous experiment to adapt to the plant deviation, and the sensor signal estimation with the adaptive $\boldsymbol{p}$ results in better estimation than the results with the fixed $\boldsymbol{p}$. Figures 15 and 16 show the fault-tolerant control results in the case of load increase. The residual signal r is omitted since the same results shown in Fig. 10 are observed.

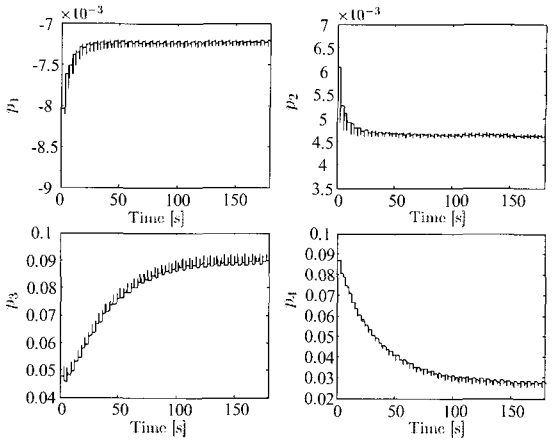

Fig. 13 Transition of $\boldsymbol{p}$ (with unknown load)

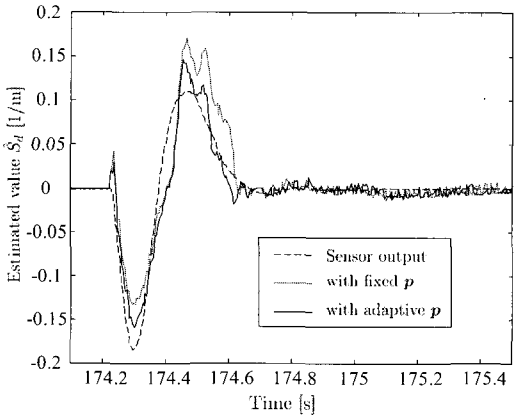

Fig. 14 Sensor signal estimation result (with unknown

The control results with the adaptive $\boldsymbol{p}$ show better control performance, especially in vibration suppression, than that with the fixed $\boldsymbol{p}$. These results show that the parameter adaptation maintains the estimation accuracy of S_d and prevents the control performance degradation after fault occurrence even if plant deviations exist.

5. Conclusion

In this paper, we proposed a fault-tolerant control system with a sensor signal observer for the strain gauge sensor fault. In the proposed system, the strain gauge sensor fault is detected by monitoring the estimation error between the sensor signal and the estimated signal, and the control system works with the estimated signal after fault detection. To construct the sensor signal observer, we

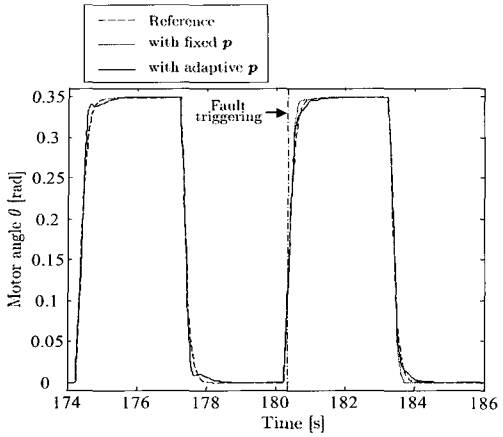

Fig. 15 Motor angle θ (with unknown load)

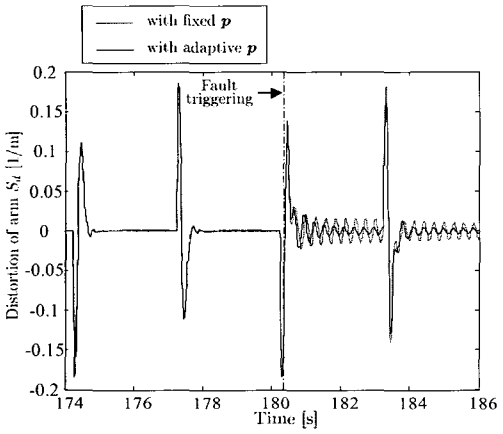

Fig. 16 Distortion of arm S_d (with unknown load)

showed the relationship between the reaction force and the strain gauge sensor signal and constructed the sensor signal observer consisting of the reaction force observer and the gain. Moreover, estimation accuracy and estimation robustness against parameter variations are improved by introducing adaptive parameters. Stability and control performance are maintained by switching from the normal-mode controller to the fault-mode controller that is designed to take into account the estimation error and the estimation delay. Loop Shaping Design Procedure (LSDP) is adopted to design the normal-mode and the fault-mode controllers, and both controllers are designed according to the same procedure, except for specifying the different W_2 in consideration of the estimation error and the estimation delay. As a result, it is possible to design a fault-mode controller easily in comparison to constructing another sensor-less control system instead of the fault-mode controller.

From some experimental results, we confirmed that the proposed control system could maintain the stability and the control performance after the strain gauge sensor fault. Estimation accuracy and control performance were improved introducing adaptive parameters with an unknown load.

References

[1] Hayato Komatsu, Tatsuya Suzuki, Shigeru Okuma, and Yasuhiro Yamaguchi, "Realization of Fault Tolerant Design Control for the Re-entry Space Vehicle Using μ-synthesis", in Proc. Technical Meeting on Industrial Instrumentation and Control IEEJ, 2002, IIC-02-28, pp.77~81(in Japanese).

[2] Yoshiro Hamada, Seiichi Shin, and Noboru Sebe, "A Design Method for Fault-Tolerant Multivariable Control Systems ---A Condition for *l*-partial Integrity---", SICE Trans., Vol. 34, No. 9, pp.1184~1190, Sep. 1998(in Japanese).

[3] Rolf Isermann, Ralf Schwarz, and Stefan stölzl , "Fault-Tolerant Drive-by-Wire Systems", IEEE Control Systems Magazine, Vol. 22, No. 5, pp.64~81, Oct. 2002.

[4] Atsushi Inoue, Satoshi Komada, and Takamasa Hori, "Control of Flexible Arms by Bending Moment Considering Second Mode Vibration", in Proc. national convention record IEEJ industry applications society, 1999 pp.403~404(in Japanese).

[5] Kazuaki Yuki, Toshiyuki Murakami, and Kouhei Ohnishi, "Vibration Control of a 2 Mass Resonant System by the Resonance Ratio Control", IEEJ Trans. Industry Applications, Vol. 113-D, No. 10, pp.1162~1169, Oct. 1993 (in Japanese).

[6] Kiyoshi Ohishi, Masaru Miyazaki, and Masahiro Fujita, "Hybrid Position and Force Control without Force Sensor" RSJ Journal., Vol. 11, No. 3, pp.468--476, Apr. 1993(in Japanese).

[7] Satoshi Komada, Kenji Ohta, Muneaki Ishida, and Takamasa Hori, "Trajectory Control of Flexible Arms Using Vibration Suppression Control by First Order Lag Strain Signal Feedback", in Proc. the 2nd Asian Control Conference, 1997, pp.185~188.

[8] Takashi Suzuki, "Adaptive Control", CORONA PUBLISHING CO., LTD, Tokyo, Japan, 2001, pp.87~90 (in Japanese).

[9] Duncan McFarlane, and Keith Glover, "A Loop Shaping Design Procedure Using H_∞ Synthesis", IEEE Trans.

Automatic Control, Vol. 37, No. 6, pp.759~769, Jun. 1992.

[10] Hayato Komatsu, Tadanao Zanma, Tatsuya Suzuki, and Shigeru Okuma, "Switching of H_∞ Controllers under Constraints and Decision of Controller State at Instance of the Controller Switching", IEEJ Trans. Electronics, Information and Systems Society, Vol. 121-C, No. 12, pp.1897~1904, Dec. 2001(in Japanese).

[11] Xianchun DING, and Paul M. FRANK, "Fault detection via factorization approach", Systems and Control Letters, Vol. 14, issue5, pp.431~436, Jun. 1990.

[12] Yu Izumikawa, Kazuhiro Yubai, and Takamasa Hori, "Vibration Suppression Control of Flexible Arm Robot by PD Gain Switching Considering Sensor Failure", in Proc. 2002 IEEE International Conference on Industrial Technology, pp.684~689, 2002.

Yu Izumikawa received his B.E., and M.E. degrees in the Department of Electrical and Electronic Engineering from Mie University, Mie, Japan, in 2000, and 2002, respectively. His research interests include fault detection, and fault-tolerant control.

Kazuhiro Yubai received his B.E., M.E., and Ph.D. degrees in Electrical Engineering from Nagoya University, Nagoya, Japan, in 1996, 1998, and 2000, respectively. He is currently a Research Associate at Mie University. His research interests include robust control, system identification, and motion control.

Junji Hirai was born in Sizuoka Pref., Japan, on Oct. 27, 1951. He received his B.S. degree in Electrical Engineering from the University of Tokyo in 1976. He received his Ph.D. degree from Yokohama National University, Japan in 1999. He joined the Yasukawa Electric Corporation, Japan, in 1982, and moved to Mie University in 2002, where he is presently a Professor in the E & E Department. His fields of interest include power electronics, motion control and robotics. Dr. Hirai is a member of the Institute of Electrical Engineer of Japan.